A Novel Microspheres Composite Hydrogels Cross-linked by Methacrylated Gelatin Nanoparticles, Enhanced Mechanical Property and Biocompatibility

C. H. Wang[1], C. D. Mu[2] and W. Lin[1]

1 Department of Biomass and Leather Engineering, Key Laboratory of Leather Chemistry and Engineering of Ministry of Education, Sichuan University, Chengdu, Sichuan, China .610065.

2 Department of Pharmaceutics and Bioengineering, School of Chemical Engineering, Sichuan University, Chengdu, China, 610065.

a) Corresponding author, wlin@scu.edu.cn

b) wangchunhua@scu.edu.cn

Abstract. We report a novel macromolecular microsphere composites (MMC) hydrogel based on polyacrylamide with enhanced mechanical property and biocompatibility. The key feature of our approach is the use of prepared methacrylated gelatin nanoparticles (MA-GNP) as the cross-linker, which have the ability of chemical crosslinking by the polymerization of C=C bonds, such that the composite hydrogels can be formed by radical polymerization of acrylamide (AAm) on the surface of MA-GNP. The smooth spherical particles with an average size of ~100 nm have been synthesized through a modified two-step desolvation method as proved by atomic force microscopy (AFM). The results of nuclear magnetic resonance and dynamic light scattering further confirm the presence of reactive groups (C=C bonds) in the particles and its narrow sizes distribution. The resulting composite hydrogels (MA-GNP/PAAm) are porous materials with tunable pore sizes and exhibit enhanced compressive resistance and elasticity as well. Increasing appropriately the dosage of MA-GNP reduces the equilibrium swelling ratio and improves thermal stability of the gels. Moreover, all the hydrogels exhibit prolonged blood-clotting time, nonhemolytic nature and strong suitability for cell proliferation, indicating the improved antithrombogenicity and excellent cyto-compatibility. It suggests that the novel MA-GNP/PAAm hydrogels have potential application as tissue engineer scaffold materials, and the MA-GNP can be a promising macromolecular microsphere cross-linker for application in biomedical materials.

1 Introduction

Polymer hydrogels are non-water soluble materials with a hydrophilic three-dimensional crosslinking network structure and exhibit unique properties such as excellent permeability, high water absorptivity, good elasticity and biocompatibility. To date, hydrogels have been widely used in biomedical applications including contact lenses[1], wound dressings[2], tissue engineering materials[3] and drug delivery[4]. Nevertheless, the non-uniform cross-linking structures in the conventional hydrogels lead to poor mechanical property, which greatly limits their practical applications.

To toughen the gels, great efforts have been made to fabricate new kinds of polymer hydrogels[5,6,7]. One of the novel and important developments is macromolecular microsphere composite (MMC) hydrogels with well-defined structures, first proposed by Wang and coworkers in 2007[8]. In this hydrogel, the macromolecular microspheres act as crosslinking points and the uniform polymer chains are chemically grafted onto the microspheres. This unique microstructure can endow the MMC hydrogels with high mechanical strength and excellent resilience because the applied force can be evenly distributed by all polymer chains[9]. In contract to the preparation of nanocomposite (NC) hydrogel made from specific polymers with a kind of water swellable clay, the synthesis of MMC hydrogels is a general and facile strategy. It only requires organic components and the compositions and properties of the hydrogels can be tailored by changing the microspheres and monomers. Moreover, the surface structure of organic microspheres can be more easily designed as required, compared with the inorganic particles used in NC systems.

So far, MMC gels have received considerable interest[10,11], and the formation mechanism[12,13], the relationship between network structure and property[14-16] have also been explored. However, most of microspheres used in the MMC hydrogels are mainly synthetic polymer such as polystyrene (PS) or poly(styrene-cobutylacrylate) particles. Only a few reports have used the biodegradable starch-based microspheres for synthesis of MMC hydrogels[10], but without any evaluation of the hydrogels for bio-related applications. Biocompatibility is one of the essential characteristics of hydrogels used in biomedical applications. Therefore, the fabrication of MMC hydrogels with good biocompatibility and mechanical properties is highly desirable.

Gelatin has exhibited significance in biomedicine and food filed as it offers the advantages of excellent biocompatibility, biodegradability and low immunogenicity. In our previous works, the introduction of gelatin and methacrylamide-modified gelatin (MA-gelatin) into clay-polyacrylamide (PAAm) NC gels could substantially improve the biocompatibility of gels[17,18]. However, the incompatibility of gelatin polyelectrolyte and clay limit the improvement both in mechanical property and biocompatibility of the gels. Inspired by the MMC hydrogels, it is believed that sole introduction of the gelatin-based microspheres into the PAAm is expected to strength the AAm hydrogels while simultaneously keeping the enhanced biocompatibility.

Hence, in this work a novel microsphere composite hydrogel with both good biocompatibility and enhanced mechanical properties has been prepared by using acrylamide (AAm) as the monomer and MA-gelatin nanoparticles (MA-GNP) as cross-linker. Herein, MA-gelatin is chosen instead of gelatin for the fabrication of the described nanoparticles because it not only can retain the good biocompatibility and hydrophilicity of gelatin[19,20] but also has the possibility of chemical crosslinking due to the presence of reactive C=C bonds, in contrast to unmodified gelatin[21]. Therefore, the obtained biocompatible particles containing C=C bonds can be expected to be as an effective cross-linker and modifier due to the combined processes of polymerization and crosslinking during the synthesis of MMC hydrogels. Our aim is to prepare a novel microsphere composite hydrogel with the potential for wound dressings and tissue engineer scaffold materials.

2 Experimental Section

2.1 Materials

Acrylamide, gelatin (type B, ~240 Bloom), glutaraldehyde (50% aqueous solution), methacrylic anhydride (MA), 2,4,6-trinitro-Benzenesulfonicacid (TNBS) and glycine (AR) were purchased from Aladdin Inc. Ammonium persulfate (APS), acetone and N,N,N',N'-tetramethylenediamine (TEMED) were obtained from Sigma-Aldrich. The concentrations of the stock solutions of TEMED and APS were fixed at 10% v/v and 3% w/v, respectively. L929 cells were obtained from Chinese Academy of Science Cell Bank for Type Culture Collection (Shanghai, China). Dulbecco's modified Eagle's medium (DMEM) were purchased from Hyclone (USA), penicillin and astreptomycin were purchased from Gibco (USA). Cell counting kit-8 (CCK8) was purchased from Kumamoto (Japan).

For the present study, the free amino groups of gelatin B were quantitatively measured by the Habeeb method[22] with glycine solutions (the phosphate buffer as a solvent, pH 7.4) in various concentrations as standard. According to the calibration curve (R^2=0.9998), the amount of free amino groups of the gelatin was 0.355 mmol g^{-1}, this value is consistent with previous study[23].

2.2 Sample preparation

2.2.1 Preparation of Methacrylated gelatin (MA-gelatin)

Methacrylated gelatin (MA-gelatin) was prepared by the reaction between gelatin and methacrylic anhydride, as previously reported23. Detailedly, 5 g gelatin (~1.775 mmol free amino groups) was dissolved in 50 mL phosphate buffer (PBS, pH 7.4, 0.2M) at 50 °C f for 1.5 h. Then 0.2~0.6 mL MA (1.30~3.90 mmol) was added dropwise under vigorously stirring at 2500 rpm, respectively and the reaction was allowed to proceed for 3 h. Subsequently the mixture was diluted with 100 mL PBS and dialyzed against deionized water at 40 °C for 24 h to remove the excess MA and other impurities. The resulting MA-gelatin was obtained as a white solid after lyophilization. The degree of substitution (DS) of MA-gelatin is defined as the percentage of ε-amino groups of gelatin that are modified and determined by Habeeb method[22]. Briefly, the reaction of TNBS and free amino groups at 40 °C led to a trinitrobenzene compound, and the optical absorbance of the solution was recorded with UV-Vis spectrophotometer at 415 nm. The DS of MA-gelatin was calculated using the following equation:

$$OD\ (\%) = \frac{OD_{\mathrm{g}} - OD_{\mathrm{m}}}{OD_{\mathrm{g}}} \times 100 \qquad (1)$$

where ODg and ODm are the optical density (OD) values of gelatin and MA-gelatin, respectively.

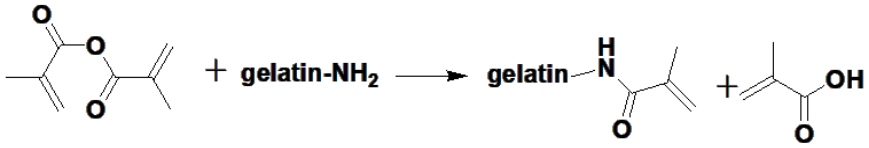

Scheme 1. Schematic representation of methacrylamide modification reactions yielding MA-gelatin.

2.2.2 Preparation of methacrylated gelatin nanoparticles (MA-GNP).

The MA-GNP was prepared from DS50% MA-gelatin crosslinked with glutaraldehyde by a modified two-step desolvation method, previously described by the group of Coester [24]. Typically, 1.25 g MA-gelatin was dissolved in 25 mL distilled water under constant heating (T=40 °C) and stirring. Then 25 mL of a desolvating agent (acetone) was added to the solution to obtain the high-molecular-weight (HMW) gelatin. After that, the HMW-gelatin was redissolved in 25 mL distilled water and the pH of the solution was adjusted to 12.0. The gelatin was then desolvated again by dropwise addition of acetone under constant heating until the mixture becomes milky white. After stirring for 10 min, glutaraldehyde solution (100 µL) was added to cross-link the particle. The reaction was conducted at 50 °C for 16h under constant stirring. Finally, the dispersion was filtered and centrifuged at 10000g (Sigma, 3-18 K) for 20 min. After the last centrifugation, the particles were dispersed in supernatant distilled water and the residual acetone was removed by slow vaporization. The resulting MA-GNP was obtained as pale-yellow particles after lyophilization.

2.2.3 Preparation of polyacrylamide based composite hydrogels (MA-GNP/PAAm) crosslinked by MA-GNP

The composite hydrogels were synthesized through in-situ free radical polymerization. The initial reaction solution consists of monomer (AAm), cross-linker (MA-GNP), initiator (KPS), and accelerator (TEMED). The molar ratio of MMA/TEMED/APS was 7/0.132/0.2/02. In all cases, the concentration of AAm were set at 10% w/v, and the mass ratio of MA-GNP to AAm was varied from 0 to 25% w/w. AAm (0.5 g) and MA-GNP (0~0.125g) were added into a glass bottle, respectively, and the total volume was fixed to 4.87 mL with deionized water. After magnetic stirring at room temperature for 2 h, the mixture solution was bubbled with nitrogen gas for 10 min, and then APS (100 µL) and TEMED (30 µL) were added. The reaction was conducted at room temperature for 24 h. The resulting gels in this study are denoted as x% MA-GNP/PAAm, where x stands for 100×MA-GNP/AAm (w/w).

2.3 Characterizations

2.3.1 Nuclear Magnetic Resonance Spectroscopy (1H-NMR)

The MA-gelatin and MA-GNP were proved by 1H-NMR spectroscopy (AV II, Bruker, Germany) [25]. 5~10 mg Samples of were dissolved in 550 µL of deuterium oxide (D_2O) before measurement. 1H-NMR spectra were collected at 35 °C and at a frequency of 600 MHz by using a Bruker AV II spectrometer.

2.3.2 Atomic force microscopy (AFM)

The particles dispersion (10 µL) at a concentration of 0.05 mg mL^{-1} was dropped onto a freshly cleaved mica substrate and dried at room temperature in a desiccator with silica gel for 24 h. The samples were scanned in air by a Dimension 3100 Nanoscope IV equipped with UrtlalveerB probes (SPM-9600, Shimadzu, Japan) in a tapping mode.

2.3.2 Particle Size measurement

The particle sizes of MA-GNP samples was measured by a Malvern Nano-ZS ZEN3600 instrument using a Zetasizer at a detection angle of 90° at 25 °C in the dust-free circumstance. The concentration of MA-GNP dispersions was 0.04 mg mL^{-1}. The mean particle size and polydispersity index were recorded in the cumulant mode employing the built-in Malvern software.

2.3.3 Fluorescence spectrum and confocal laser scanning microscopy (CLSM)

Measurement of the fluorescence spectrum of the MA-GNP particles was performed by a fluorescence spectrophotometer (F-7000, Hitachi, Japan) at 25 □C. The excitation slit was set at 10 nm and scanning speed was 30000 nm/min. The excitation wavelength was 336 nm, 488 nm and 543 nm respectively. And the range of emission spectra was 355 ~ 700 nm, 500 ~ 700 nm, 520 ~ 700 nm respectively. The concentration of MA-GNP was 0.5 mg/mL. The Fluorescence properties and distribution of particles in as-prepared hydrogels were imaged by CLSM (Nikon Eclipse TI, Nikon, Japan), and an oil mirror 40× (numerical aperture, NA = 0.85) was used. The hydrogels were directly placed on the cover slides and a series of x/y layers were scanned. The laser wavelength was 543 nm and filter wavelength was 605 nm. Three different sets of experiments were performed for each sample.

2.3.4 Scanning electron microscopy (SEM)

The morphology of the hydrogels was obtained by a scanning electron microscope (Quanta 400 FEG, FEI, USA) with operating voltage of 20 kV. The samples were first freeze-dried in lyophilizer (ALPHA 1-2 LD, Christ, Germany) for 30 h at -50 °C before observation.

2.3.5 Measurements of mechanical properties

Compressive tests of the as-prepared hydrogel samples were carried out on a MTS Universal Testing Machine (CMT6202, MTS systems Co., Ltd., China) at room temperature. The highest compressive strain was set at reach a level of 90%. At least three measurements were performed for each sample.

2.3.6 Swelling Experiments

Swelling experiments were carried out at room temperature by immersing the as-prepared hydrogels in pure deionized water and also in buffer solutions to reach swelling equilibrium, respectively. The corresponding swollen weight of the gels was recorded (Ws). After that, the swollen gels were then freeze-dried and weighted again to measure the weight of the dry gel (Wd). The effect of ionic strength on the equilibrium swelling ratio (ESR) was also investigated. The ionic strength was changed from 0 to 0.1 M at room temperature. The equilibrium swelling ratio was calculated as

$$S = \frac{W_s - W_d}{W_d} \qquad (2)$$

2.3.7 Measurements of Thermal Properties.

Thermal properties were performed on a thermogravimetric analyzer (NETZSCH TG 209F1, Selb, Germany) from 60 to 600 °C at a heating rate of 10 °C/min under a nitrogen atmosphere. All samples were freeze-dried before measurement and the mass of each sample was 4 mg.

2.3.8 Blood clotting test

The anticoagulant properties of the composite hydrogels were evaluated by the contact method and the fresh rabbit blood was extracted according to ASTM standards [26]. 0.2 mL of diluted anticoagulant acid citrate dextrose (ACD) blood was dropped on the surface of the gel samples (the diameter of gels is 30 mm and thickness is 10 mm) or glass coverslips [27] and 25 mL of $CaCl_2$ solution (0.2 mol L-1) was then added to the ACD blood to activate the clotting reaction. After incubation at 37 °C for 5 min, 50 mL deionized water was added and the incubation was continued for another 10 min to lyse the red blood cells that had not been trapped in the thrombus. The absorbance of the supernatant at 545 nm is measured by UV-vis spectrometer (Perkin-Elmer Lamda 25, Germany) to determine the concentration of free hemoglobin in the water. 0.2 mL of diluted ACD blood in 50 mL of deionized water was used as a control. The blood clotting index (BCI) was calculated according to the following equation:

$$BCI\ (\%) = \frac{OD_t \times 100}{OD_c} \qquad (3)$$

where ODt and ODc denote the OD values of test and control samples, respectively.

2.3.9 Hemolysis assay

The hemolytic potential of the MA-GNP composite hydrogels was evaluated following the reported procedure [28]. Briefly, the sterilized swollen hydrogel pieces were immersed into a glass tube with 10 mL physiological saline and the incubation was kept for 30 min at 37 °C. 0.2 mL of diluted ACD blood was then added and the mixture was incubated in a rocking shaker at 37oC for 1 h, followed by centrifugation at 2000 rpm for 5 min. The optical density of the supernatant was determined at 545 nm by a UV-vis spectrometer. Positive and negative controls were prepared by adding 0.2 mL diluted ACD blood into 10 mL deionized water or physiological saline, respectively. The percentage hemolysis was calculated as follows:

$$Hemolysis\ (\%) = \frac{(OD_t - OD_n) \times 100}{OD_p - OD_n} \qquad (4)$$

where ODt, ODn, and ODp denote the OD values of test, negative, and positive samples, respectively. The hemolysis results were average of six measurements.

2.3.10 In vitro cytotoxicity

These measurements were carried out using an indirect method in which the extracts were used to culture cells, similar as the previous report [29,30.] The stock extracts (C = 100%) of MA-GNP/PAAm gels were obtained by immersing gels (thickness >0.05 mm) of each material (3 cm^2/ mL) in Dulbecco's modified Eagle's medium (DMEM) at 37 °C for 3 days without agitation. Before cell culturing, the extract solutions were filter sterilized through a 0.22 um microporous membrane. The extract with a concentration of 50% (C = 50%) was also prepared by diluting the stock extract with equal volumes of culture medium.

(1) Activation of L929 Cells and preparation of MA-GNP/PAAm gels materials. L929 cells were cultured in petri dishes (Thermo NunclonTM, USA, 100*20 mm) using Dulbecco's modified Eagle's medium with high glucose supplemented with penicillin and streptomycin. They were maintained in a 5% CO_2 atmosphere at 37 °C (Carbon dioxide incubator, Thermo, USA) and subcultured. Cells were passaged approximately 2 times per week and the medium was exchanged every 2 days.

(2) Exposure of cells to extracts. The cells were seeded into three 96-well plates at a density of 1 × 104 cell /well per well (Corning, USA) in 0.l ml medium. After 24 h of incubation as described above to allow cell attachment, the medium was replaced with the corresponding solutions, respectively, (a) DMEM without cells, used as a blank control; (b) DMEM with cells, used as negative control; (c) 100% stock extracts (C=100%) and 50% extracts (C=50%). In order to determine the cells relative proliferation rate (RGR) at different incubation interval, the cells were cultured for 6, 24 and 48h in a humidified atmosphere with 5% CO_2 at 37 °C, respectively. After incubation, the medium was removed and replaced with 90 µL fresh DMEM and 10 µL CCK-8 assay stock solution (5 mg/mL). The cells were incubated for 80 min to allow the formation of formazan crystals, which was determined at 450 nm by a Microplate reader (550 BIO-RAD, USA). The cell relative proliferation rate (RGR) was calculated according to the following equation:

$$RGR(\%) = \frac{(OD_t - OD_b)}{(OD_n - OD_b)} \times 100 \qquad (5)$$

where OD_t, OD_n, and OD_b the OD values of test, negative, and blank samples, respectively. The RGR results were average of three measurements. And qualitative grading of cytotoxicity of the extracts are referred to ISO 10993-5 standard [31] and United States Pharmacopeia (USP)[32].

3 Results and discussion

3.1 Synthesis of MA-gelatin and MA-GNP

The presence of the methacrylate groups in the molecular structure of MA-gelatin makes it polymerizable (Figure 1a) [19]. The percentage of 3-amino groups of gelatin that are modified (namely, DS) can be adjusted by varying the amount of MA present in the initial reaction mixture (table 1). DS50% MA-gelatin is chosen for the preparation of MA-GNP as it retains amino groups for the particle synthesis and simultaneously contains carbon-carbon double bond, which can participate in subsequent radical polymerization reactions to achieve the crosslinking of PAAm gels. The modification of gelatin and synthesis of MA-GNP were verified by ^{1}H-NMR spectroscopy (Figure 1b). The signal at δ=2.8 ppm (attributed to lysine methylene groups) in the spectrum of MA-gelatin decreases with the increasing DS, indicating that the amino groups of the lysine have partially been substituted by methacrylamide groups. As for the MA-GNP, the absence of signal δ=2.8 ppm suggests that the rest of the amino groups of the lysine of MA-gelatin have almost entirely reacted with aldehyde groups of glutaraldehyde, leading to the MA-GNP. In addition, compared with unmodified gelatin, new signals observed at 5.2 ppm < δ < 5.6 ppm and at δ = 1.7 ppm both in the spectra of MA-gelatin and MA-GNP are ascribed to the acrylic protons and the methyl function of the introduced methacrylic groups, respectively [25]. It confirms the presence of C=C bonds both in MA-gelatin and MA-GNP.

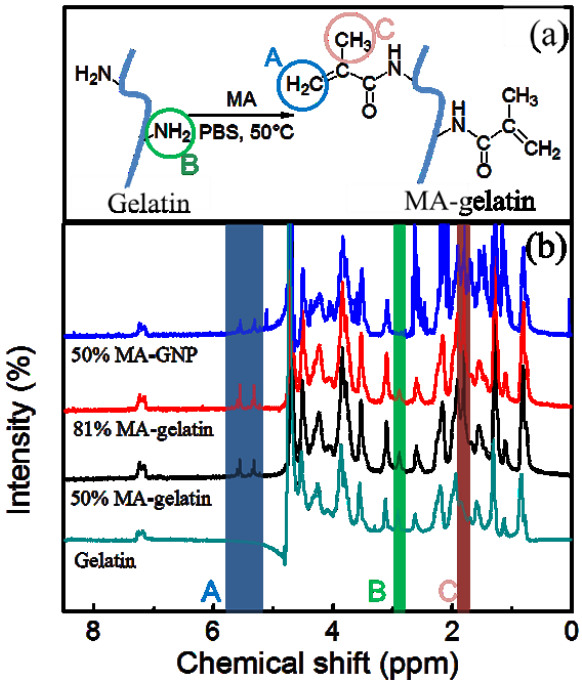

Fig. 1. (a) Schematic illustration showing the synthesis of MA-gelatin;(b) 1H NMR spectra of gelatin, MA-gelatin (DS50%, DS81%) and MA-GNP (DS50%). The signals of the acrylic protons and the methyl function of the introduced methacrylic groups are denoted as A and C, while lysine methylene signal of gelatin is denoted as B.

Table 1. Effect of the amount of MA on DS of MA-gelatin.

Dosage of MA (mL)	DS of MA-gelatin (%)
0.2	50.8±3.8
0.3	66.7±2.5
0.4	80.2±4.3
0.5	89.7±2.5
0.6	94.7±1.5

3.2 The characteristic of MA-GNP

Figure 2 shows the AFM morphology and size analysis of the synthesized particles. The nanoparticles is found to be spherical in shape with a smooth surface in a size range of 50~200 nm, fairly mono-dispersed on the mica. Studies have shown that the phase images can be used to visualize the local surface property of heterogeneous regions because the phase shift of the cantilever oscillation is very sensitive to the viscoelasticity like rigidity of the surfaces during tapping[33]. The phase graph of the particles (Figure 2b) reflects the variation of the surface property of the MA-GNP by the contrast of cores (dark) and edges (light). It reveals that the density of the MA-GNP is not homogeneous whose edge parts are looser than the cores, which agrees well with our previous results[34]. Moreover, the size distribution of the synthesized particles (Figure 2c) as measured by dynamic light scattering (DLS) further confirm that the average size of the particle is ~100 nm in diameter with a unimodal size

distribution (PDI = 0.17). The above-mentioned NMR analysis and AFM results indicate that the MA-GNP is suitable to be introduced into the microspheres hydrogel system as a cross-linking agent.

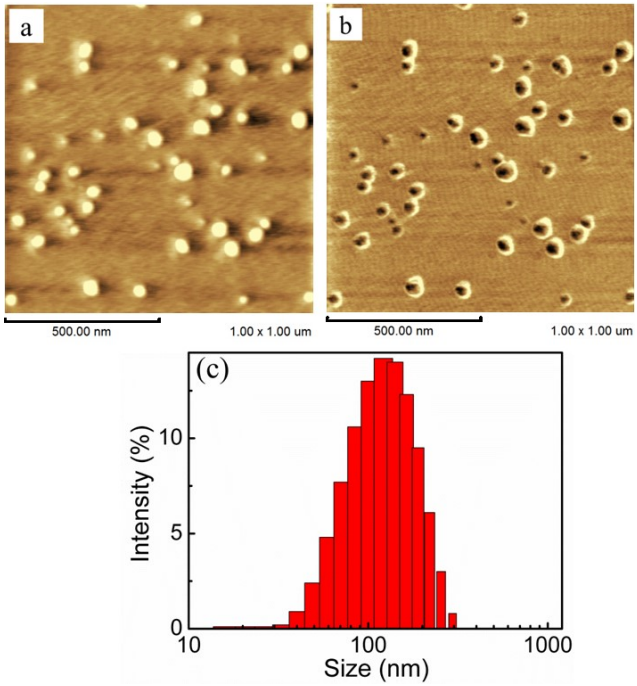

Fig. 2. (a) AFM height images of the MA-GNP, 1 μm × 1 μm; (b) Phase graph of the MA-GNP; (c) Size distributions of the MA-GNP.

3.3 Copolymerization and structure of MA-GNP composite hydrogels

Figure 3a shows the schematic illustration of the preparation process of MA-GNP/PAAm hydrogels and proposed synthesis mechanism. The crosslinking at intra- or inter-molecular chains of MA-gelatin is due to the establishment of aldimine linkages (CH=N) between the free amino groups of MA-gelatin and glutaraldehyde, which leads to the formation of MA-GNP [35]. Also, the C=C bonds of MA-GNP endow the particles with chemical crosslinking activity. Thus the microsphere composite hydrogels is formed by radical polymerization of AAm on the surface of MA-GNP (Figure 3a). The introduction of MA-GNP will change the nature of the gel network and improve various performances of the gels. When adding the pale yellow MA-GNP to the AAm solution, all of the suspensions were transparent and stable, which is favorable for the in situ polymerization (Figure 3b). The resulting composite hydrogels exhibit high transparency with yellow color. And the color of gels gradually deepen with increasing MA-GNP content.

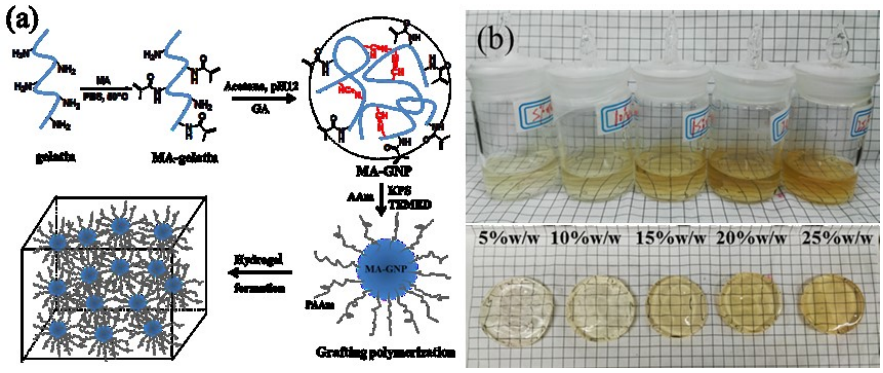

Fig. 3. (a) Proposed mechanism for the formation of an MMC hydrogel and an MMC hydrogel microstructure. (b) Mixtures solution before polymerization and resulting hydrogels composite hydrogels with different amounts of MA-GNP.

Figure 4a shows the fluorescence spectra of MA-GNP at different excitation wavelengths. For MA-GNP, the strongest emission band is observed between 420 and 480 nm (band I) upon excitation at 365 nm. And the emissions are centred at 560 nm (band II) upon excitation at 488 nm and 543 nm. The observed variations in autofluorescence relate to the different chemical structures of the MA-GNP particles. MA-GNP have two kinds of unsaturated double bonds including C=N bonds from the Schiff's base reaction and C=C bonds from MA-gelatin. Herein, the high-energy absorption (band I) is attributed to the π-π* transition of C=C double bonds and the bands II is associated with the n-π* transitions of C=N bonds in the Schiff's base [36]. The autofluorescent characteristic of MA-GNP is beneficial to see how the particles are distributed in the cross-linked hydrogel networks. Note that the strongest emission intensity of microspheres is observed upon excitation at 543 nm. Therefore, the following CLSM image of the gels (Figure 4b and 4c) is given upon excitation at 543 nm, in which the red part represents the microspheres in composite hydrogels. It demonstrates that with increasing amounts of microspheres from 5% to 20%, the crosslinking density of the composite hydrogel is increased and the distribution MA-GNP is relatively uniform in the hydrogel even at the higher content of 20%.

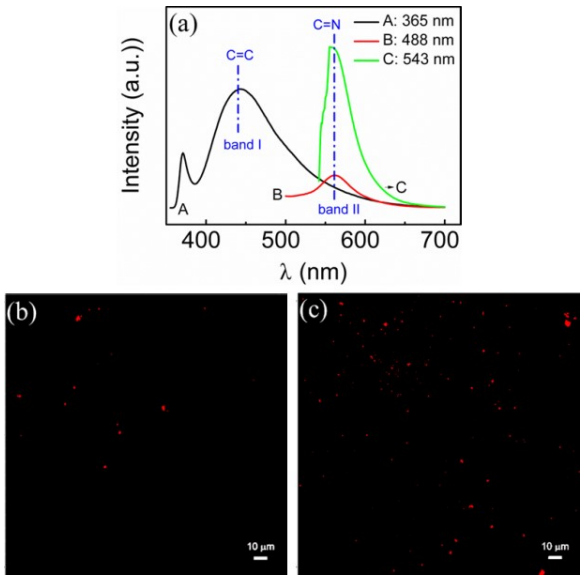

Fig. 4. (a) Fluorescence spectra of the MA-GNP at different excitation wavelengths. (b) CLSM image of 5% MA-GNP composite hydrogels. (c) CLSM image of 20% MA-GNP composite hydrogels.

The cross-sectional morphologies of the MMC hydrogels with different amounts of MA-GNP are given in Figure 5. It can be seen that, after drying and the removal of frozen water, all the gels are honeycomb-like with uniform interconnected pores due to the uniform dispersion of nanoparticles, the size of which decrease with the increasing amounts of MA-GNP. Considering the same initial gel compositions, subsequent preparation process and freeze-drying conditions, the reason for the difference in the porous structure can only be the varied amounts of cross-linkers MA-GNP and resulting crosslink density. Clearly, the lower the MA-GNP content (Figure 5b-f), the larger the pore size in the hydrogel, indicating that the porosity can be adjusted by controlling the content of the macromolecular microsphere cross-linker MA-GNP. Moreover, the pore sizes of the gels are distributed in the range of 20~200 μm, which is the ideal pore size distribution for promoting cell adhesion and proliferation such as fibroblasts [37], suggesting that the gels can be potentially used as cell scaffold materials.

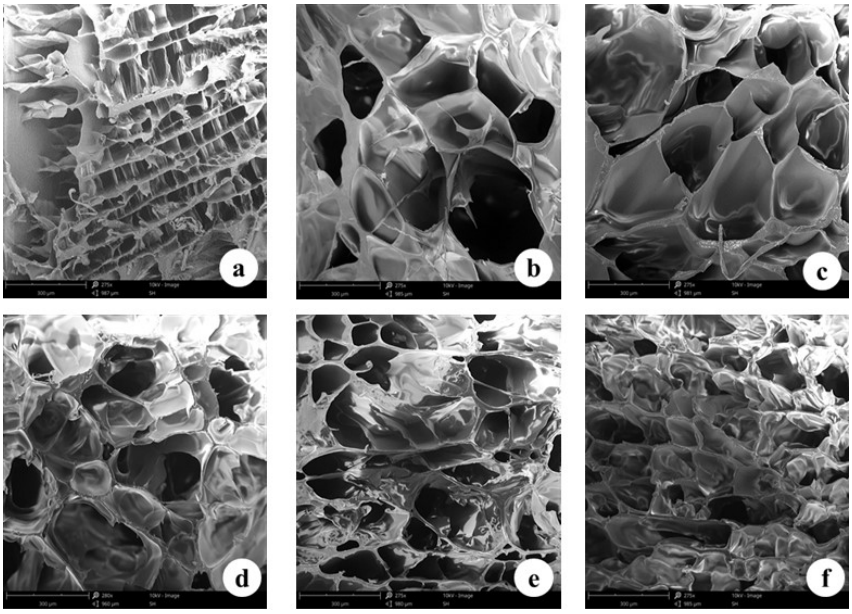

Fig. 5. SEM micrographs of composite hydrogels with different amounts of MA-GNP： (a) 0%; (b) 5%; (c) 10%; (d) 15%; (e) 20%; (g) 25%.

3.4 Mechanical properties

The compressed and stretched mechanical properties of the as-prepared MA-GNP/PAAm gels were evaluated as given in table 2 and Figure 6. Note that 5% MA-GNP/PAAm gels is viscous and its shape is destroyed after compression due to its low cross-linking degree. With the increase of cross-linker dosage(≦20%), the compressive stress and elasticity shaping ability of MA-GNP gels is enhanced and they can be compressed and recover to their original length without visible permanent deformation. Even when compressed to the strain of 90%, the gels with 10%~20% content of MA-GNP can quickly recover to more than 90% of the initial thickness without breakage, and the compression strength can reach up to 160 kPa. However, when the MA-GNP content is further increased to 25%, the mechanical property of the gels is decreased, with some broken part after compression. This is due to the fact that mechanical properties of polymer gel are relevant to the number of effective chains that sustain the force[38]. Hydrogels with appropriate dosage of cross-linker have more effective chains, and each effective chain can be loaded evenly before fracture, thus having higher mechanical properties. Compared with typical MA-gelatin crosslinked hydrogels[18] with enhanced mechanical property but at the sacrifice of elasticity, the MA-gelatin nanoparticles crosslinked gels can sustain higher compressive strain while simultaneously exhibiting better deformation restorability. It is possibly attributed to the uniform chemical crosslinking and the long flexible chains between crosslinks MA-gelatin particles[8]. The compressive stress–strain test reveals that the macromolecular microsphere cross-linker, MA-GNP, can improve the rigidity of the hydrogel network while keeping the good elasticity. In addition, the 10% MA-GNP gels can sustain bending stretching and knotting, as shown in Figure 7. The gels can be stretched at least 500% in length without breakage. The results indicate that the MA-GNP/PAAm gels are a flexible and elastic material.

Table 2. Photographs of an MMC hydrogel during the compression test.

	5%w/w	15%w/w	25%w/w
original state	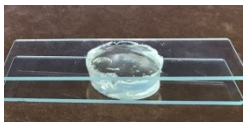	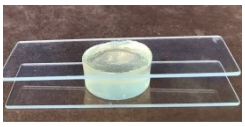	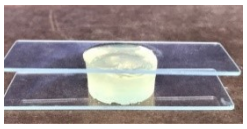
compressed state	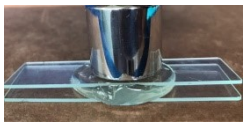		
recovery state	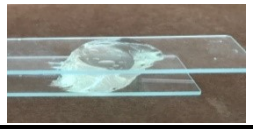	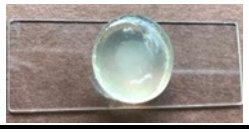	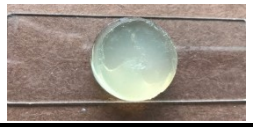

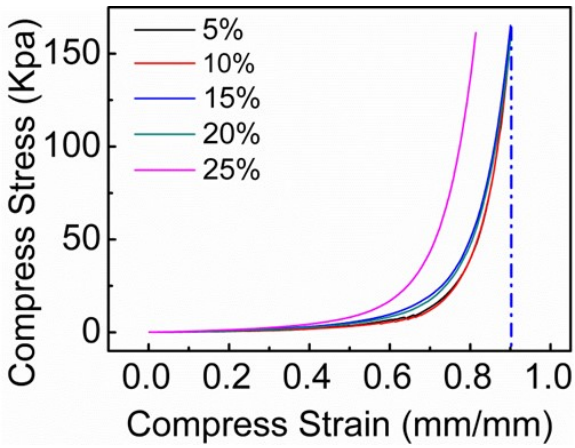

Fig. 6. Compression stress-strain curves of composite hydrogels with different amounts of MA-GNP.

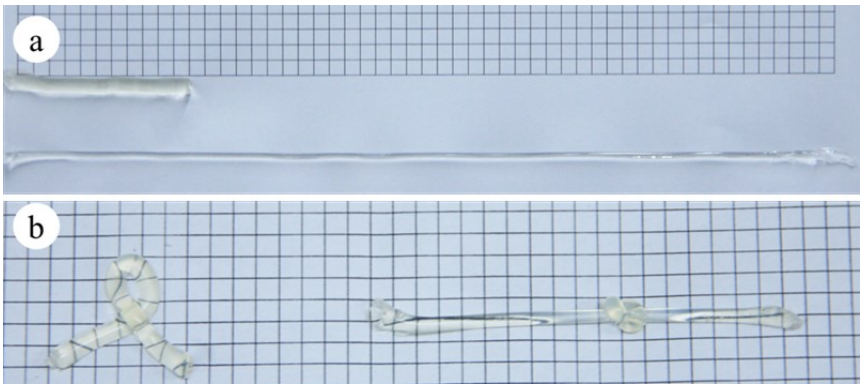

Fig. 7. Optical images showing the process of the 10% MA-GNP composite hydrogels, (a)being stretched; (b) bending and knotting state.

3.5 Swelling Behaviors

The swelling behavior of the hydrogels are investigated at room temperature in solutions of various ionic strength ranging from 0 to 0.1 M. Figure 8 shows that the equilibrium swelling ratio of the gels decreases with increasing ionic strength of the solution. It can be ascribed to the reduction in the osmotic pressure difference between the hydrogels and the external solution with increasing ionic

strength [39]. Note that the MMC gels with lower MA-GNP contents have higher water absorption, which owes to the fact that a lower MA-GNP content means a less cross-linked network structure and thus more free space available for shrinking in the resulting MMC gels. However, when the MA-GNP content is further increased from 20% to 25%, the ESR is instead increased, which possibly relate to the hydrophilicity of the excessive MA-GNP inhomogeneously distributed in the gels.

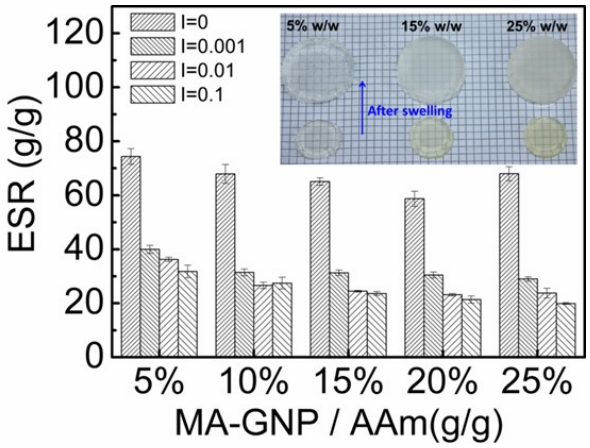

Fig. 8. Effects of ionic strength on the equilibrium swelling ratio of composite hydrogels with different amounts of MA-GNP.

3.6 Thermal properties

Figure 9 shows the thermal properties of the MMC gels as measured by thermogravimetric analysis (TGA). For all prepared MMC gels, there were three decomposition stages, ranging from 60 to 600 °C. The first stage (stage II) occurring between 50 and 150 °C is attributed to the removal of bound water[17]. The second degradation stage from 200 to 320 °C (stage II) is mainly associated with loss of ammonia with formation of imide groups through cyclization[40]. The third decomposition stage in the range of 320 to 500 °C (stage III) mainly corresponds to the decomposition of the polymer chains[41]. The position of maximum decomposition temperature corresponding to stage I, stage II and Stage III for hydrogel samples (Table 3) all shift to higher temperature with increasing the content of MA-GNPs, indicating the enhanced thermal property. This is reasonable because MA-GNPs nanoparticles act as a cross-linker in MMC gels and can effectively enhance the cross-link density of the hydrogel network.

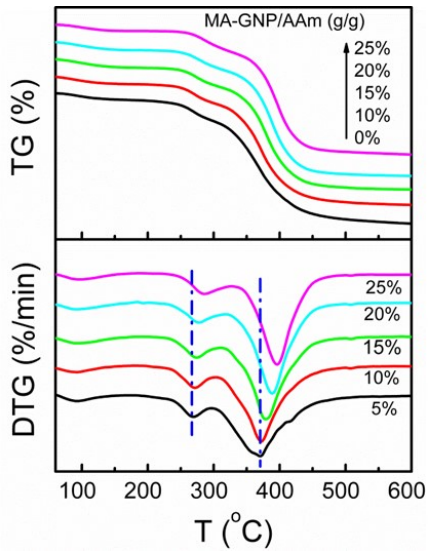

Fig. 9. The TG-DTG curves of composite hydrogels with different amounts of MA-GNP.

Table 3. The maximum decomposition temperature corresponding to stage I, stage II and Stage III of the Hydrogel Samples.

m_{MA-GNP}/m_{AAm}(g/g)	Stage I / °C	Stage II / °C	Stage III / °C
5%	92.3	268.3	371.1
10%	92.4	270.8	371.1
15%	92.4	273.4	378.5
20%	92.3	278.4	388.6
25%	97.7	285.9	396.5

3.7 In vitro blood compatibility

The blood compatibility of materials is very important as it plays a key role in determining their utility for bio-medical applications. A thrombosis or hemolytic reaction is undesirable but frequently occurs when foreign materials come into contact with blood [18,42]. Therefore, the in vitro blood compatibility of MA-GNP gels is evaluated in terms of the blood clotting index (BCI) and degree of hemolysis. The BCI of hydrogels with different amounts of MA-GNP are shown in Figure 10a. It is recognized that a higher value of blood clotting index indicates a better antithrombogenicity [43]. The results show that BCI of all the MA-GNP gels can reach up to 70%, significantly higher than glass surface (45%). This is quite expected because of the well-known biocompatible nature of gelatin, which can effectively inhibit the platelet adhesion and thrombus formation [44,45]. And our results confirm that MA-GNP can also retain this feature. Note that increasing MA-GNP can improve the BCI, but the 15% MA-GNP/PAAm hydrogel has the highest BCI. This result is possibly related to the combined consequence of the increase in the crosslink density of the network and the decreased water uptake capacity of gels, caused by increasing the content of cross-linker (MA-GNP). The surface with enhanced stiffness and smoothness and higher hydrophilicity may offer less interaction between the materials and the blood components [46], thus enhancing the blood compatibility of the polymeric hydrogels. Figure 10b shows the degree of erythrolysis and hemoglobin dissociation in contact with MA-GNP gels at 37 °C for 60 min. The hemolytic ratios for all the MA-GNP gels are below the international permissible level of 5%, indicating they are nonhemolytic [28].

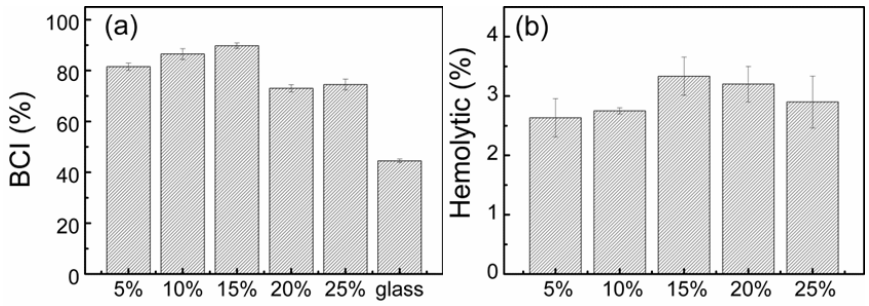

Fig. 10. (a) The BCI of composite hydrogels with different amounts of MA-GNP. (b) The haemolysis of composite hydrogels with different amounts of MA-GNP.

3.8 In vitro cytotoxicity

L929 cells are mouse fibroblasts with fusiform or flat stellate and protuberant, as shown in Figure 11a, and this kind of cell can be sub-cultured with the advantage of stability and repeatability. L929 cells after digestion with trypsin are wrinkled and rounded, as shown in Figure 11b. The results of the cell viability test of hydrogels are shown in Figure 11c and Figure 11d. And RGR of the L929 cells in the diluted extract and stock extract of hydrogels of all the samples for different incubation time (6-48h) are more than 85%, which achieve a numerical grade lower than 100%, indicating that all the MA-GNP/PAAm hydrogels exhibit good cytocompatibility[31,32].

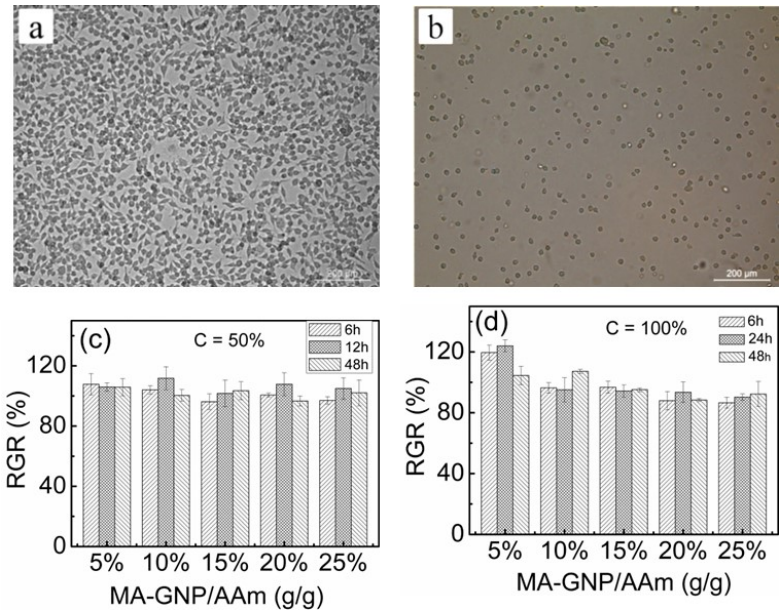

Fig. 11. (a) Images of adherent covered L929 cell, (b) images of digested L929 cell, (c) RGR in the 50% extracts of the gels, (d) RGR in 100% extracts of the gels.

4 Conclusions

In conclusion, this study introduces a general and facile route to fabricate novel microsphere composite hydrogel with good mechanical properties and biocompatibility. The smooth and spherical MA-GNP with an average size of 100 nm was obtained by the modified two-step desolvation process. It is can be readily introduced into the PAAm hydrogels system as a cross-linker to prepare MMC hydrogels via a free radical polymerization reaction with acrylamide monomers. The results show the MA-GNP/PAAm gels are materials with uniform interconnected pores and the pore size can be adjusted by the dosage of gelatin. Compared with the MA-gelatin crosslinked systems, the crosslinking action of MA-GNP nanoparticles can improve both the compressive resistance and the elasticity of PAAm hydrogels. The hydrogels exhibit good water absorption and the swelling property is influenced by cross-linker dosage and ionic strength. Moreover, with increasing cross-linker dosage, the thermal stability of the composite hydrogel is improved distinctly. Most importantly, all the MA-GNP gels have enhanced blood compatibility endowed by MA-GNP and the extracts of MA-GNP hydrogels have no toxic side effect on cells. The present work not only exploits new strategies to fabricate MMC hydrogels but also advance the potential application of biodegradable gelatin-based nanoparticles in biomedical fields.

References

1. *Maulvi, F. A., Lakdawala, D. H., Shaikh, A. A., Desai, A. R., Choksi, H. H., Vaidya, R. J. In vitro and in vivo evaluation of novel implantation technology in hydrogel contact lenses for controlled drug delivery. J. Control. Release, 226, 47-56, 2016*
2. *Singh, B., Sharma, S., Dhiman, A. Acacia gum polysaccharide based hydrogel wound dressings, Synthesis, characterization, drug delivery and biomedical properties. Carbohyd. Polym., 165, 294-303, 2017*
3. *Lam, J., Clark, E. C., Fong, E. L., Lee, E. J., Lu, S., Tabata, Y. Evaluation of cell-laden polyelectrolyte hydrogels incorporating poly (l-Lysine) for applications in cartilage tissue engineering. Biomaterials 2016, 83, 332-346, 2016*
4. *Seeli, D. S., Prabaharan, M. Guar gum oleate-graft-poly (methacrylic acid) hydrogel as a colon-specific controlled drug delivery carrier. Carbohyd. Polym., 158, 51-57, 2017*
5. *Okumura, Y., Ito, K. The Polyrotaxane Gel, A Topological Gel by Figure-of-Eight Cross-links. Adv. Mater., 13(7), 485-487, 2001*
6. *Gong, J. P. Why are double network hydrogels so tough? Soft Matter, 6(12), 2583-25902010*
7. *Gaharwar A K, Peppas N A, Khademhosseini A. Nanocomposite hydrogels for biomedical applications. Biotechnol. Bioeng., 111(3), 441-453, 2014*
8. *Huang, T., Xu, H., Jiao, K., Zhu, L., Brown, H., Wang, H. A novel hydrogel with high mechanical strength, a macromolecular microsphere composite hydrogels. Adv. Mater., 19(12), 1622-1626, 2007*
9. *Jiang, F., Huang, T., He, C., Brown, H. R., Wang, H. Interactions Affecting the Mechanical Properties of Macromolecular Microsphere Composite Hydrogels. J. Phys. Chem. B, 2013, 117(43), 13679-13687.*
10. *Tan Y, Xu, Wang P, Li, W. Sun, S., Dong, L. S. High mechanical strength and rapid response rate of poly(n-isopropyl acrylamide) hydrogel crosslinked by starch-based nanospheres. Soft Matter, 6(7), 1467-1471, 2010*
11. *Liu, C., Tan, Y., Xu, K., Li, Y., Lu, C., Wang, P. Synthesis of poly(2-(2-methoxyethoxy)ethyl methacrylate) hydrogel using starch-based nanosphere cross-linkers. Carbohyd. Polym. 105(6), 270-275, 2014*
12. *Zhai, D., Zhang, H. Investigation on the application of the TDGL equation in macromolecular microsphere composite hydrogel. Soft Matter, 9(3), 820-825, 2012*
13. *Li, X., Ji, G., Zhang, H. Phase transitions of macromolecular microsphere composite hydrogels based on the stochastic Cahn–Hilliard equation. J. Comput. Phys. 283, 81-97, 2015*
14. *Jiang, F., Huang, T., He, C., Brown, H. R., Wang, H. Interactions Affecting the Mechanical Properties of Macromolecular Microsphere Composite Hydrogels. J. Phys. Chem. B, 117(43), 13679-13687, 2013*
15. *Wu, Y., Zhou, Z., Fan, Q., Chen, L., Zhu, M. Facile in-situ fabrication of novel organic nanoparticle hydrogels with excellent mechanical properties. J. Mater. Chem., 19(39), 7340-7346, 2009*
16. *Zhang, H. Strain-stress relation in macromolecular microsphere composite hydrogel. Appl. Math. Mech-Eng., 37(11),1539-1550, 2016*
17. *Li, C., Mu, C., Lin, W., Ngai, T. Gelatin Effects on the Physicochemical and Hemocompatible Properties of Gelatin/PAAm/Laponite Nanocomposite Hydrogels. Acs Appl. Mater. Inter., 7(33),18732-18741, 2015*
18. *Li, C., Mu, C., Lin, W. Novel Hemocompatible Nanocompsite Hydrogels Crosslinked with Methacrylated Gelatin. Rsc Adv., 6(49), 43663-43671, 2016*
19. *Nichol, J. W., Koshy, S., Bae, H., Chang, M. H., Yamanlar, S., Khademhosseini, A. Cell-laden microengineered gelatin methacrylate hydrogels. Biomaterials, 31(21), 5536-5544, 2010*
20. *Benton, J. A., Deforest, C. A., Vivekanandan, V., Anseth, K. S. Photocrosslinking of gelatin macromers to synthesize porous hydrogels that promote valvular interstitial cell function. Tissue Eng. Part A., 15(11), 3221-3230, 2009*
21. *Dragusin, D. M., Van Vlierberghe, S., Dubruel, P., Dierick, M., Van Hoorebeke, L., Declercq, H. A. Novel gelatin–PHEMA porous scaffolds for tissue engineering applications. Soft Matter, 8(37), 9589-9602, 2012.*
22. *Habeeb, A. F. S. A. Determination of free amino groups in proteins by trinitrobenzenesulfonic acid. Anal. Biochem., 14(3), 328-336, 1966*
23. *Bulcke A. V. D, Bogdanov, B., Rooze, N. D., Schacht, E. H., Cornelissen, M., Berghmans, H. Structural and rheological properties of methacrylamide modified gelatin hydrogels. Biomacromolecules, 1(1), 31-38, 2000*
24. *Coester, C. J., Langer, K., Van, B. H., Kreuter, J. Gelatin nanoparticles by two step desolvation a new preparation method, surface modifications and cell uptake. J. microencapsul., 17(2), 187-193, 2000*
25. *Hoch, E. Hirth, T., Tovar, G. E. M., Borchers, K. Chemical tailoring of gelatin to adjust its chemical and physical properties for functional bioprinting. J. Mater. Chem. B., 1(41), 5675-5685, 2013*
26. *Standard test methode for haemolysis of materials. ASTM-F90; ASTM international, West Conshohocken, United states, 1990.*
27. *Cui, L., Tang, C., Yin, C. Effects of quaternization and PEGylation on the biocompatibility, enzymatic degradability and antioxidant activity of chitosan derivatives. Carbohyd. Polym., 87(4), 2505-2511, 2012*
28. *Meng, Z. X., Zheng, W., Li, L., Zheng, Y. F. Fabrication and characterization of three-dimensional nanofiber membrance of PCL–MWCNTs by electrospinning. Mater. Sci. Eng. C, 30(7), 1014-1021, 2010*
29. *ISO 10993-12, 2007–Biological evaluation of medical devices–Part 12, Sample preparation and reference materials.*
30. *Ciapetti G, Granchi D, Stea S,. Savarino, L. Verri, E. Gori, A. Savioli, F. Montanaro, L. Cytotoxicity testing of materials with limited in vivo exposure is affected by the duration of cell-material contact. J. biomed. Mater. Res., 1998, 42(4), 485-490, 1998*
31. *Cytotoxicity Biological Evaluation of Medical Devices – Part 5, Tests for In Vitro Cytotoxicity. Australian Standard™, AS ISO 10993.5–2002, 2002*

32. *Anon. Biological reactivity tests in vitro, In United States Pharmacopeia. 24th revision. United States Pharmacopeial Convention, Inc., Rockville, Maryland, 2014, pp 1813–1831*
33. *Ishida, N., Inoue, T., Minoru Miyahara, A., Higashitani, K. Nano bubbles on a hydrophobic surface in water observed by tapping-mode atomic force microscopy. Langmuir., 16(16), 6377-6380, 2000.*
34. *Tan, H., Sun, G., Lin, W., Mu, C. Ngai, T. Gelatin particle-stabilized high internal phase emulsions as nutraceutical containers. Acs Appl. Mater. Inter., 2014, 6(16),13977-13982.*
35. *Kesavan, S., Bai. S. A. Effect of surfactant on the release of ciprofloxacin from gelatin microspheres. Ars pharm, 51(1), 1-16, 2010*
36. *Wei, W., Wang, L. Y., Yuan, L., Wei, Q., Yang, X. D., Su, Z. G. Preparation and application of novel microspheres possessing auto-fluorescent properties. Adv. Funct. Mater., 17(16), 3153-3158, 2007*
37. *Ma, L., Gao, C., Mao, Z., Zhou, J., Shen, J., Hu, X. Collagen/chitosan porous scaffolds with improved biostability for skin tissue engineering. Biomaterials, 24(26), 4833-4841, 2003*
38. *Itagaki, H., Kurokawa, T., Furukawa, H., Nakajima, T. Katsumoto, Y. Gong, J. P. Water-induced brittle-ductile transition of double network hydrogels. Macromolecules, 43(22), 9495-9500, 2010*
39. *Raafat, A. I. Gelatin based pH-sensitive hydrogels for colon-specific oral drug delivery, Synthesis, characterization, and in vitro release study. J. Appl. Polym. Sci., 118(5), 2642–2649, 2010*
40. *Nayak, B. R., Singh, R. P. Development of graft copolymer flocculating agents based on hydroxypropyl guar gum and acrylamide. J. Appl. Polym. Sci., 81(7), 1776-1785, 2001*
41. *Zhou, C., Wu, Q. A novel polyacrylamide nanocomposite hydrogels reinforced with natural chitosan nanofibers. Colloid. Surface. B. 84(1), 155-162, 2011.*
42. *Menzies, K. L., Jones, L. The impact of contact angle on the biocompatibility of biomaterials. Optometry Vision Sci. 87(6), 387-399, 2010.*
43. *Shankarraman, V., Davis-Gorman, G., Copeland, J. G., Caplan, M. R., Mcdonagh, P. F. Standardized methods to quantify thrombogenicity of blood-contacting materials via thromboelastography. J. Biom. Mater. Res. B, 100(1), 230-238, 2012*
44. *Tabuchi N, De, H. J., Gallandat, H. R. C., Boonstra, P. W., Van, O. W. Gelatin use impairs platelet adhesion during cardiac surgery. Thrombosis and haemostasis, 74(6), 1447-1451, 1995*
45. *Ren, J., Jin, W., Hong, S., Nan, H. Surface modification of polyethylene terephthalate with albumin and gelatin for improvement of anticoagulation and endothelialization. Appl. Surface Sci., 255(2), 263-266, 2008*
46. *Bajpai, A. K., Sharma, M. Preparation and characterization of novel pH-sensitive binary grafted polymeric blends of gelatin and poly(vinyl alcohol), Water sorption and blood compatibility study. J. Appl. Polym. Sci., 100(1), 599-617, 2010.*